JOURNAL OF OPTOELECTRONICS AND ADVANCED MATERIALS Vol. 12, No. 8, August 2010, p. 1758 - 1764

Dye-sensitized nanocrystalline TiO_2 films based on Pechini sol-gel method using PEG with different molecular weights

G. LIANG[a], J. XU[b], W. XU[b*], X. SHEN[b], H. ZHANG[b], M. YAO[c]
[a]*College of Materials Science & Engineering, Xi'an Jiao tong University, Xi'an 710049, China*
[b]*Wuhan Textile University, Wuhan 430073, China*
[c]*Xi'an Polytechnic University Xi'an 710049, China*

Mesoporous titanium oxide (TiO_2) films were prepared based on nanocrystalline TiO_2 powder (Degussa P25) and Pechini sol-gel method by introducing polyethylene glycols (PEG) with different molecular weights. The films based on longer PEG segments showed the bigger pores and looser structures, which led to higher dye adsorption but bigger interfacial resistance. The optimized performance of the assembled dye-sensitized solar cells (DSSCs) was obtained with PEG of $\overline{M}_w$=1000, yielding short-circuit photocurrent density (J_{sc}) of 6.22 mA/cm^2, open-circuit photovoltage (V_{oc}) of 0.691 V and conversion efficiency (η) of 4.05 %, under the use of polyethylene oxide (PEO) gel electrolyte.

(Received June 28, 2010; accepted August 12, 2010)

Keywords: Dye-sensitized solar cells, TiO_2 films, PEG, Pechini sol-gel method

1. Introduction

With the increasingly serious energy-demanding and environmental-concerning, dye-sensitized solar cells (DSSCs) have attracted widespread attention due to their high photo-to-electric efficiency and low-cost manufacturing [1-5]. Generally, the DSSCs consist of two electrodes (one is the sintered nano-crystalline TiO_2 photoanode sensitized by dyes as electron transporter and the other is the platinized counter electrode for electron collection) and the electrolyte containing an iodide/tri-iodide (I^-/I_3^-) redox couple, sandwiched in between the electrodes as hole transporter. A widely recognized working mechanism of DSSCs is as follows [1]: when illuminated, the dye molecules attached on the TiO_2 films are excited via absorption of sunlight, followed by electron injection from the excited-state into the conduction band of TiO_2. The electron is then transported to the external circuit from the nanostructured TiO_2 film. From this point of view, the high surface area of the TiO_2 film as well as the good connections between the TiO_2/TiO_2 gains and TiO_2/transparent conductive oxide (TCO) glass interface are essential to the performance of DSSCs, because the light absorption related to dye loading and the electron transfer process are decided by the two factors, respectively.

Many modifications on the TiO_2 films have been carried out to satisfy the abovementioned requirements. Doohun Kim et al. [6] replaced the conventional nanocrystalline TiO_2 particles with bamboo-type TiO_2 nanotubes and Keat G. Ong et al. [7] used the highly ordered TiO_2 nanotube arrays to prepare the TiO_2 films with high surface area. P. Wang et al. [8] formed the multilayered TiO_2 films via fourfold layer deposition of TiO_2 paste and $TiCl_4$ solution, where the resulted small-sized TiO_2 particles gave rise to good connections between the TiO_2/TiO_2 gains and TiO_2/transparent conductive oxide (TCO) glass interface. These outlined methods all could effectively improve the performance of DSSCs. However, either the difficult preparation techniques of the TiO_2 nanotubes or the complex multistep coating process of the TiO_2 paste would limit their large-scale application. Recently, U. Opara Krašovec and coworkers [9, 10] developed a novel TiO_2 paste based on nanocrystalline TiO_2 powders and Pechini sol-gel method by using titanium isopropoxide ($Ti(iOPr)_4$), citric acid and ethylene glycol (EG) as precursors and obtained the TiO_2 layers with high inner surface area as well as well-connected nanocrystalline grains. The light-to-electric performance of the DSSCs assembled with these TiO_2 layers and liquid electrolytes is comparable to those obtained based on the fourfold TiO_2 layer. In this work, polyethylene glycol (PEG) with different molecular weights ($\overline{M}_w$= 400, 1000 and 2000) were introduced to the TiO_2 paste precursor to prepare the TiO_2 films based on the Pechini method. The structures and morphologies of the films were investigated by scanning electron microscopy (SEM) and X-ray diffraction (XRD). The performance of the assembled DSSCs based on the films and the polyethylene oxide (PEO) gel electrolyte has been

evaluated.

Pechini method-based TiO_2 film involves the basic domain formed by the TiO_2 nanoparticles and the close domain consisting of small-sized TiO_2 particles. As shown in Fig.1, the small-sized TiO_2 particles resulted from sintering of polytitanium ester networks which were generated from polyesterification reactions between citric acid-chelated titanate and PEG. Meanwhile, the thermal decomposition of the polyester would form the mesopores in the film, the size of which would be related to the length of PEG segments to some extent.

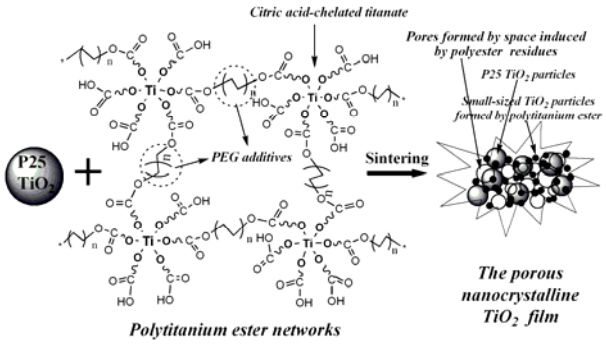

Fig.1 Schematic diagram of the formation of porous nanocrystalline TiO_2 film with P25 particles and PEG additives, based on Pechini sol-gel method.

2. Experimental

2.1. Materials

Ethylene glycol ($\overline{M}_w$ = 62), polyethylene glycol ($\overline{M}_w$ = 400, 1000 and 2000), citric acid and titanium isopropoxide were all A. R. grade (Sinopharm Chemical Reagent Co. Ltd, China) and were used as received. TiO_2 powders (P25, mean size of around 25 nm) were gained from Degussa AG, Germany. Sensitizing dye cis-bis (isothiocyanate)-bis (2, 2-bipyridine-4, 4-dicarboxylate) ruthenium (N3) was purchased from SOLARO-NIX. Fluorine doped tin oxide over-layer conducting glass (FTO glass, sheet resistance 15 Ω/cm^2) was purchased from Libbey Owens Ford Industries, USA.

2.2. Preparation of titanium dioxide thin films

The first step in TiO_2 paste preparation was synthesis of a polyester-based titanium sol (polytitanium ester networks) using a precursor with the molar ratio of 1:6:24 [$Ti(iOPr)_4$: citric acid: PEG ($\overline{M}_w$ = 62, 400, 1000 and 2000)]. Then, the TiO_2 paste was prepared by mixing the TiO_2 powder (P25) and sol (the molar ratio between the TiO_2 powder and $Ti(iOPr)_4$ was 7:1) in mortar grinder for 1 hour. Finally, the paste was deposited on the FTO conducting glass and was sintered at 450℃ for 1 hour to form the TiO_2 films. On the whole, the preparation process of the TiO_2 films, based on the Pechini sol-gel method, includes three steps as displayed in the Scheme. The P25 TiO_2 particles constituted the basic domain and the resulted small-sized TiO_2 particles formed the close domain of the films. The details of the method were described in Ref. 9.

The TiO_2 film prepared with the paste containing P25 TiO_2 powders, acetylacetone and detergent (TritonX-100), under annealing for 30 min at 450℃ [2], was used as the original reference.

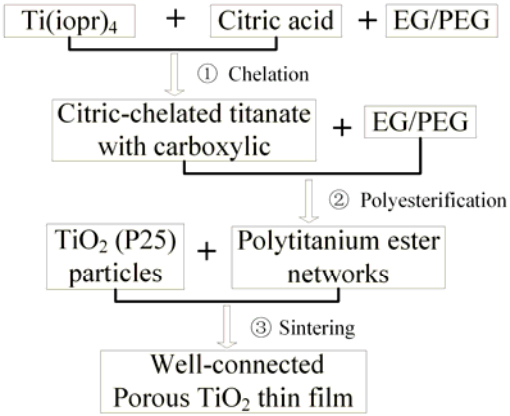

Scheme. The flow chart of preparation of TiO_2 thin film through Pechini sol-gel method.

2.3. DSSCs fabrication

The TiO_2 films were immersed in N3 solution of 0.3mM in ethanol for 24 hours. The prepared PEO-based gel electrolyte (0.8g PEO, 0.224g LiI and 0.03g I_2 in 4ml acetonitrile) was casted onto the sensitized TiO_2 electrode and then a platinum counter electrode was pressed on top of the TiO_2 electrode to form a DSSC. The effective area of the cell was 0.5 cm^2 [11].

2.4. Characterization

Scanning electron microscopy (SEM) analysis was carried out with a HITACHI X-650 microscope at 10 kV acceleration voltage after gold coating.

The X-Ray diffraction analysis was carried out on an analytical X-ray powder diffractometer (Rigaku, Japan D/Max-RB-ray, wavelength = 1.54 Å, Cu Kα radiation) with 40 kV generator intensity and 50 mA generator current. The sample was scanned from $2\theta = 10 \sim 60°$ in steps of 0.02°.

The UVPC-2550 (Shimadzu Corporation, Kyoto, Japan) was used to evaluate the dye adsorbance of the sensitized TiO_2 films. For measurement, the test dye solution was prepared by dilution of the N3 dyes in deionized water, after desorption of the dyes from the TiO_2 film in a 0.1 M NaOH solution for 12 hours.

The photocurrent and photovoltage of the cells were measured in an electrochemical workstation analyzer

(model LK9805) by a two-electrode arrangement. A 500-W Xenon lamp served as light source. The incident light density (P_{in}) was 60mW/cm^2, monitored by an irradiatometer. During irradiance and characterization, the cells were covered with a black mask fitting the active area of the cell. Based on the I-V curve, the fill factor (ff) and photo-to-electric conversion efficiency (η) of cells are defined as:

$$ff = (I_{\max} \times V_{\max}) / (I_{sc} \times V_{oc}) \quad (1)$$

$$\eta = (I_{sc} \times V_{oc} \times ff) / P_{in} \quad (2)$$

Where, I_{max} and V_{max} are the photocurrent and photovoltage for the maximum power output, I_{sc} and V_{oc} are the short-circuit photocurrent and open-circuit photovoltage of DSSCs, respectively.

3. Results and discussion

3.1. SEM studies

The SEM pictures of the TiO_2 films are presented in Fig.2. The high-magnification images of Fig.2(a)1 ~ (e)1 show all the films are composed of uniform spherical TiO_2 nanoparticles with the size of about 20 nm. The TiO_2 nanoparticles are homogenously distributed within the films without agglomeration. The connections between the grains in the films (b) ~ (e) are improved, compared with the film (a), suggesting that the $Ti(iOPr)_4$ added into the paste acts as a binder connecting the TiO_2 grains in the film. The low-magnification images of Fig.2(b)2 ~ (e)2 show that as the molecular weight of PEG increases from $\overline{M}_w$ = 62 to 400, 1000 and 2000, the pore size in the films (b) ~ (e) grows from about 0.2 μm to 0.5, 1 and 2 μm, while the porosity rises in turn, revealing the looser and looser structures of the TiO_2 films. The variation tendency of the pores in the films could be attributed to the extension of residual space between TiO_2 grains caused by thermal decomposition of the polyester composed of longer PEG segments, which act as the bridged linkage for the titanium salts (shown in Fig.1).

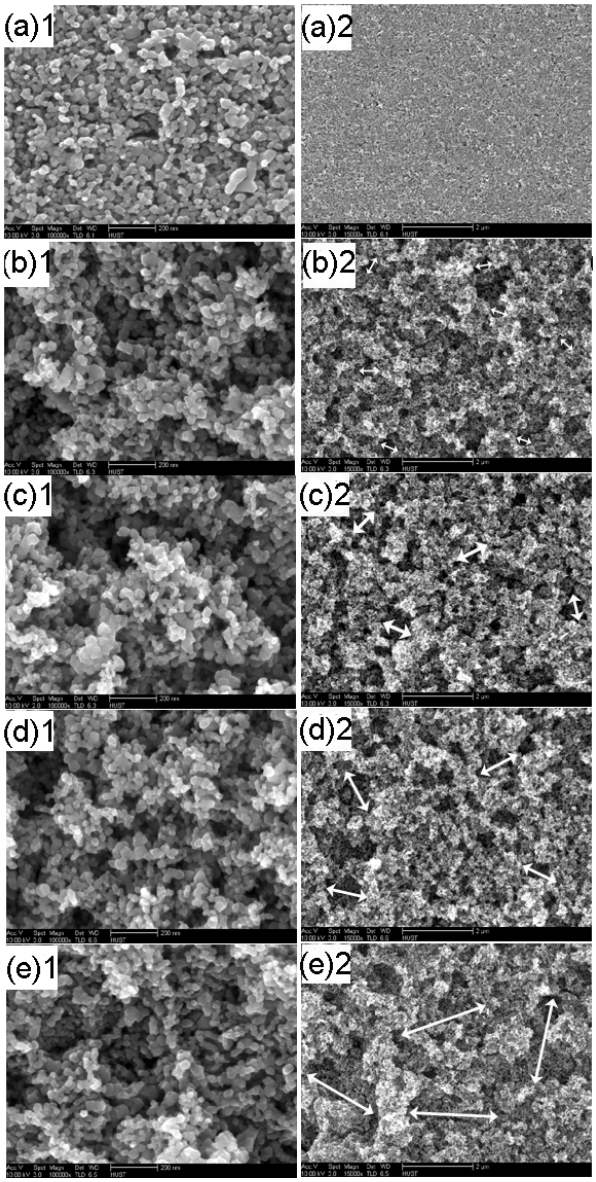

Fig.2 SEM images (first column:×15000, second: ×100000) of TiO_2 films (a) original reference, and films prepared with additives: (b) EG, (c) PEG400, (d) PEG1000 and (e) PEG2000.

3.2. X-ray diffraction

Fig.3 displays the XRD patterns of the TiO_2 films prepared with different PEG additives, where (101), (110), (004), (200), (105) and (211) reflections, corresponding to 2θ= 25.4, 27.4, 37.7, 47.9, 54.0 and 55.0°, clearly show the crystalline structure of TiO_2 films: the anatase accompanied by slight rutile phase for all the TiO_2 samples [12]. The weight ratio between anatase and rutile phases of TiO_2 in all the films (a) ~ (e) remains similar, according to the results calculated from Eq (3) [13]:

$$w(A)\% = \frac{1}{1+1.265\times I_R/I_A}\times 100\% \quad (3)$$

Where, I_A and I_R represent the intensity of the maximum diffraction peaks of anatase (2θ= 25.4°) and rutile phase (2θ= 27.4°), respectively. This indicates the PEG additives with different molecular weights almost do not influence the ratio of crystal phase of TiO_2 after sintering.

The average crystallite size P was estimated using a peak at 2θ= 25.4°, with Scherrer's equation [14]:

$$P = k\lambda/(\beta\cdot\cos\theta) \quad (4)$$

where, k ($k = 0.89$ or 1) is a constant and its value is related to several aspects, including the shape of the crystal, the Miller index of the reflecting crystallographic planes and crystallite shape, β is full width at half maximum intensity of the reflection in radians, θ is the Bragg's angle, and λ ($\lambda_{Cu k\alpha}$=1.5405 Å) is the wavelength of the X-ray radiation. The calculated values are 23.7, 19.6, 21.8, 21.2 and 22.4 nm for the reference sample and the samples with EG, PEG400, PEG1000 and PEG2000, respectively, as listed in Table 1. The crystallite sizes of the samples based on Pechini method are smaller than that of the original reference, which could be related to the generation of the small-sized TiO_2 particles through $Ti(iOPr)_4$ hydrolysis.

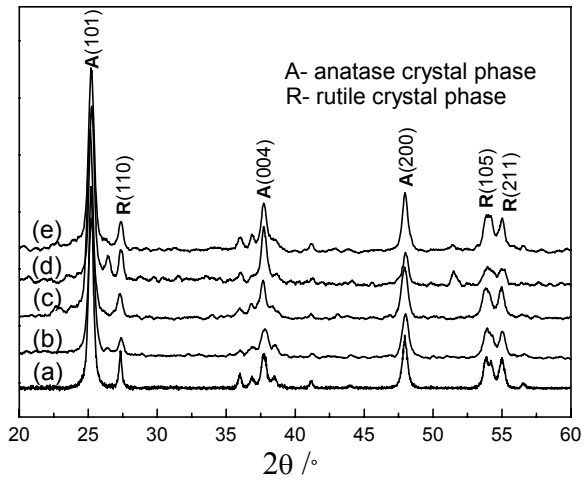

Fig. 3 XRD results of of TiO_2 films (a) original reference, and films prepared with additives : (b) EG, (c) PEG400, (d) PEG1000 and (e) PEG2000, annealed at 450℃ for 1hour.

Table 1. XRD results of TiO_2 thin films prepared by Pechini sol-gel method..

Samples	2θ (°)	hkl	Crystal phase	Width (°)	Weight ratio[a] (%)	P[b] (nm)
Original[c]	25.4°	(101)	Anatase	0.34	81.8% Anatase	23.7
	27.4°	(110)	Rutile	0.36	18.2% Rutile	
	37.7°	(004)	Anatase	0.44		
	47.9°	(200)	Anatase	0.41		
	54.0°	(105)	Rutile	0.80		
	55.0°	(211)	Rutile	0.51		
EG	25.4°	(101)	Anatase	0.41	83.4% Anatase	19.6
	27.4°	(110)	Rutile	0.34	16.6% Rutile	
	37.7°	(004)	Anatase	0.56		
	47.9°	(200)	Anatase	0.56		
	54.0°	(105)	Rutile	0.76		
	55.0°	(211)	Rutile	0.53		

Samples	2θ (°)	hkl	Crystal phase	Width (°)	Weight ratio[a] (%)	P[b] (nm)
PEG400	25.4°	(101)	Anatase	0.37	82.3% Anatase 17.7% Rutile	21.8
	27.4°	(110)	Rutile	0.35		
	37.7°	(004)	Anatase	0.42		
	47.9°	(200)	Anatase	0.60		
	54.0°	(105)	Rutile	0.71		
	55.0°	(211)	Rutile	0.50		
PEG1000	25.4°	(101)	Anatase	0.38	82.5% Anatase 17.5% Rutile	21.2
	27.4°	(110)	Rutile	0.37		
	37.7°	(004)	Anatase	0.47		
	47.9°	(200)	Anatase	0.51		
	54.0°	(105)	Rutile	0.70		
	55.0°	(211)	Rutile	0.52		
PEG2000	25.4°	(101)	Anatase	0.36	83.7% Anatase 16.3% Rutile	22.4
	27.4°	(110)	Rutile	0.37		
	37.7°	(004)	Anatase	0.42		
	47.9°	(200)	Anatase	0.58		
	54.0°	(105)	Rutile	0.76		
	55.0°	(211)	Rutile	0.53		

a The calculated weight ratio between anatase and rutile phases of TiO_2 by XRD results.
b The calculated average crystallite size of TiO_2 partical at a peak of 2θ= 25.4°.
c The film prepared according to the Ref. 2, used as the reference sample.

3.3. Dye loading

The absorbency of N3 solutions desorbed from sensitized TiO_2 films were shown in Fig.4. The two relatively sharp peaks located at 363 nm and 478 nm correspond to the characteristic absorption of N3 dye molecules [2]. The amount of the dye molecules attached to the surface of the TiO_2 films is proportional to the absorbency of the dye solutions, according to the Lambert-Beer formula. The normalized absorbency (using the absorbency of original sample (a) as reference) of the dyes rises gradually with the increased molecular weight of PEG, as shown in Fig.4b, indicating the amount of the N3 dyes adsorbed on the TiO_2 surface increases with the molecular weight of PEG additives. These results can be attributed to the higher porosity (proved by the SEM results) and the larger inner surface area of the TiO_2 films prepared with the longer PEG segments.

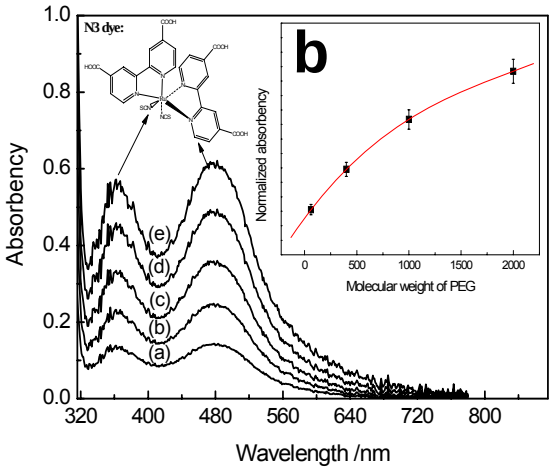

Fig. 4 The absorbency of N3 dyes desorbed from sensitized TiO_2 films (a) original reference, and films prepared with additives: (b) EG, (c) PEG400, (d) PEG1000 and (e) PEG2000.

3.4. Photoelectric performance

In order to evaluate the influence of different morphology of the TiO_2 films induced by the PEG additives on the photoelectric performance of DSSCs, the photocurrent-voltage curves for cells fabricated with the TiO_2 films and PEO-based gel electrolyte were tested under a light intensity of 60mW/cm^2 (top curves) and in a dark environment (bottom curves), as given in Fig.5. The corresponding parameters of photoelectric properties of DSSCs are listed in table 2. The values of the short-circuit current densities (J_{SC}) are 5.13, 5.73, 6.22 and 6.53 mA/cm^2 for the original film and the films prepared with PEG400, PEG1000 and PEG2000, respectively. The J_{SC} of the Pechini method-based films are much higher than that of the original film, indicating the modification of the TiO_2 paste with the Pechini method improves the efficiency of the DSSCs. Additionally, the value of J_{SC} increases with the molecular weight of PEG, which can be attributed to the increased dye loading of the films. The open-circuit voltage (V_{oc}) of the original reference film is 0.602 V and the values rise to 0.636, 0.691 and 0.668 V for the films based on PEG400, PEG1000 and PEG2000, respectively. The increase of V_{oc} for the Pechini method-based films could be assigned to the good connections between the TiO_2 grains caused by the $Ti(iOPr)_4$ hydrolysis, when compared with the original film; whereas, the following decline of the V_{oc} from the PEG1000-based film to the PEG2000-based film is ascribed to the increase of the interfacial impedance (confirmed by the increased dark currents of the films in Fig.5b) due to the much looser structure of the latter. As the results, the conversion efficiency (η) of the cells first increases and then decreases, and the optimized performance is obtained with PEG of $\overline{M}_w$=1000.

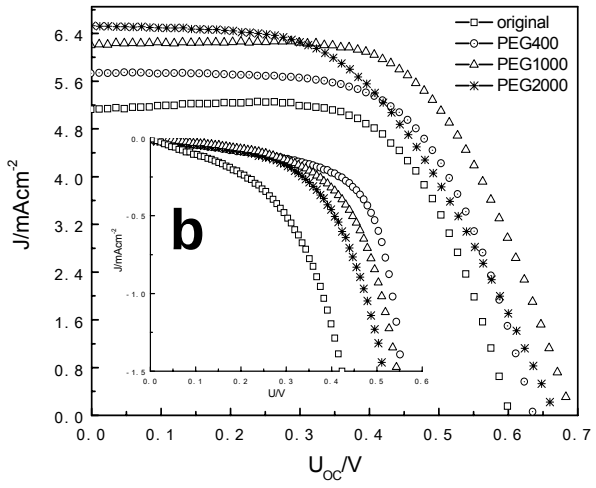

Fig. 5 The photocurrent-voltage curves of DSSCs.

Table 2 The parameters of photoelectric properties of DSSCs.

	J_{SC} (mA/cm^2)	V_{OC} (V)	ff	η^b (%)
Original[a]	5.13	0.602	0.61	3.29
PEG400	5.73	0.636	0.62	3.75
PEG1000	6.22	0.691	0.64	4.05
PEG2000	6.53	0.668	0.51	3.68

a The TiO_2 paste prepared according to literature cite 2.
b The conversion efficiency of assembled DSSCs based on PEO gel electrolyte, under a light intensity of 60mW/cm^2, the active area for the tested cell is 0.5 cm^2.

4. Conclusions

The mesoporous TiO_2 films were prepared by addition of PEG with different molecular weights into the TiO_2 paste via Pechini sol-gel method. The porosity of the films increase with the increasing of molecular weight of PEG, which leads to the increased dye loading as well as the enlarged interfacial resistance. As the results, the optimized performance of the assembled DSSCs was obtained with PEG of $\overline{M}_w$=1000, yielding short-curcirt photocurrent density (J_{sc}) of 6.22 mA/cm^2, open-circuit photovoltage (V_{oc}) of 0.691 V and conversion efficiency (η) of 4.05 %.

Acknowledgements

This work was financially supported by the Key Project of Science and Technology Research of Ministry of Education (No. 208089), the Natural Science Foundation of Hubei Province (No. 2007ABA075 and No.2008CDB261) and the Educational Commission of Hubei Province (Q20101606).

References

[1] B. Oregan, M. Gratzel, Nature **353**, 737 (1991).
[2] M.K. Nazeeruddin, A. Kay, I. Rodicio, R. Humphrybaker, E. Muller, P. Liska, N. Vlachopoulos, M. Gratzel, J. Am. Chem. Soc. **115**, 6382 (1993).
[3] U. Bach, D. Lupo, P. Comte, J. E. Moser, F. Weissortel, J. Salbeck, H. Spreitzer, M. Gratzel, Nature **395**, 583 (1998).
[4] C. I. Oprea, F. Moscalu, A. Dumbrava, S. Ioannou, A. Nicolaides, M. A. Girtu, J. Optoelectron. Adv. Mater. **11**, 1773 (2009).

[5] A. Diacon, E. Rusen, C. Boscornea, C. Zaharia, C. Cincu, J. Optoelectron. Adv. Mater. **12**, 199 (2010).
[6] D. Kim, A. Ghicov, S.P. Albu, P. Schmuki, J. Am. Chem. Soc. **130**, 16454 (2008).
[7] C. A. Grimes, K. G.. Ong, O. K. Varghese, G.. K. Mor, K. Shankar, Sol. Energy Mater. Sol. Cells **91**, 250 (2007).
[8] P. Wang, S.M. Zakeeruddin, P. Comte, R. Charvet, R. Humphry-Baker, M. Gratzel, J. Phys. Chem. B **107**, 14336 (2003).
[9] U. O. Krasovec, M. Berginc, M. Hocevar, M. Topic, Sol. Energy Mater. Sol. Cells **93**, 379 (2009).
[10] M. Hocevar, U.O. Krasovec, M. Berginc, G. Drazic, N. Hauptman, M. Topic, J. Sol-Gel Sci. Technol. **48**, 156 (2008).
[11] X. L. Shen, W. L. Xu, J. Xu, G. J. Liang, H. J. Yang, M. Yao, Solid State Ion. **179**, 2027 (2008).
[12] B. Orel, A.S. Vuk, R. Jese, M. Gaberscek, G. Drazic, Sol. Energy Mater. Sol. Cells **90**, 452 (2006).
[13] R. A. Spurr, H. Myers, Anal. Chem. **29**, 760 (1957).
[14] J. Xu, Q. Xiong, G.J. Liang, X.L. Shen, H. T. Zhou, W.L. Xu, J. Macromol. Sci. Part B-Phys. 856 (2009)

*Corresponding author: weilin-xu@hotmail.com; lgj511011@163.com